ADVANCED FUNCTIONAL MATERIALS

FULL PAPER

DOI: 10.1002/adfm.200500569

Luminescence of Functionalized Carbon Nanotubes as a Tool to Monitor Bundle Formation and Dissociation in Water: The Effect of Plasmid-DNA Complexation**

By *Lara Lacerda*, *Giorgia Pastorin*, *Wei Wu*, *Maurizio Prato*, *Alberto Bianco*, and *Kostas Kostarelos**

Functionalized carbon nanotubes (f-CNTs) are explored as novel nanomaterials for biomedical applications. UV-vis luminescence of aqueous dispersions of CNT–NH_3^+ and CNT–NH–Ac (NH–Ac: acetamido) is observed using standard laboratory spectrophotometric instrumentation, and the measured fluorescence intensity is correlated with the aggregation state of the f-CNTs: a high intensity indicates improved f-CNT individualization and dispersion, while a decrease in fluorescence intensity indicates a higher degree of nanotube aggregation and bundling as a result of varying the sodium dodecyl sulfate (SDS) concentrations and pH in the aqueous phase. Moreover, utilization of this relationship between fluorescence intensity and the state of f-CNT aggregation is carried out to elucidate the interactions between f-CNTs and gene-encoding plasmid DNA (pDNA). pDNA is shown to interact with CNT–NH_3^+ primarily through electrostatic interactions that lead concomitantly to a higher degree of f-CNT bundling. The CNT–NH_3^+/pDNA interactions are successfully competed by SDS/f-CNT surface interactions, resulting in the displacement of pDNA. These studies provide exemplification of the use of fluorescence spectrophotometry to accurately describe the aggregation state of water-soluble f-CNTs. Characterization of the complexes between pDNA and f-CNTs elucidates the opportunities and limitations of such supramolecular systems as potential vectors for gene transfer.

1. Introduction

Since their discovery in 1991,[1] carbon nanotubes (CNTs) have been extensively explored for numerous applications. Their unique structural, electronic, and mechanical properties[2] have attracted the attention of researchers to this innovative material and its potential for applications in field emission, energy storage, molecular electronics, and biomedicine.[3] Characterization of CNTs dispersed in liquid phases was possible after overcoming the hurdle of insolubility in organic and aqueous solvents through functionalization.[4] However, in the aqueous phase, individual CNTs tend to aggregate readily in bundles that are difficult to suspend effectively as a consequence of strong van der Waals forces.[5]

Attempts to disperse individual CNTs in solvents involve the reduction of the short-range attractions between neighboring nanotubes through the introduction of repulsive forces.[6] This is commonly achieved by sonication of CNT bundles in the presence of polymers,[6] surfactants,[7] peptides,[8] or single-stranded DNA (ssDNA).[9] This leads to stable dispersions of less-aggregated CNTs as a result of wrapping and coating of the surfactant or macromolecule around the CNTs. An alternative approach is the introduction of electrostatic repulsive forces by covalent attachment of charged groups on the nanotube surface, which reportedly leads to the dissociation of CNT bundles.[10] Georgakilas et al.[4] have attached a short alkyl chain with terminal ammonium groups on the sidewalls of single-walled CNTs (SWNTs) and multiwalled CNTs (MWNTs), achieving adequate aqueous solubility and improving the dispersity of CNTs. Such aqueous dispersions of CNTs consequently allow for exploration of their use in biological and biomedical applications.

Our group has recently shown that positively charged f-CNTs can deliver plasmid DNA (pDNA) into mammalian (human) cells for gene-transfer applications.[11] Moreover, we have been exploring the complexation characteristics between f-CNTs and double-stranded pDNA (ds-pDNA), and their impact on the gene-expression capabilities of those newly designed gene-delivery vector systems.[12] Other groups have investigated the effects of covalent and noncovalent conjugation of ssDNA onto CNTs for a variety of different applications, including the development of microcircuits,[13] biosensors,[14] probe tips for atomic force mi-

[*] Dr. K. Kostarelos, L. Lacerda
Centre for Drug Delivery Research, The School of Pharmacy
University of London
29–39 Brunswick Square, London WC1N 1AX (UK)
E-mail: kostas.kostarelos@pharmacy.ac.uk
Dr. G. Pastorin, Dr. W. Wu, Dr. A. Bianco
Immunologie et Chimie Thérapeutiques
Institut de Biologie Moléculaire et Cellulaire
UPR9021 CNRS, 67084 Strasburg (France)
Prof. M. Prato
Dipartimento di Scienze Farmaceutiche
Università di Trieste
34127 Trieste (Italy)

[**] This work was financially supported by the School of Pharmacy, University of London, CNRS, the University of Trieste, and MIUR (PRIN 2004, prot. 2004035502). W. W. and G. P. are grateful to the French Ministry for Research and New Technologies for post-doctoral fellowships (GenHomme Network 2003). L. L. acknowledges the Portuguese Foundation for Science and Technology (FCT/MCES) for the award of a PhD fellowship (Ref.: SFRH/BD/21845/2005).

croscopy (AFM),[15] and for improving the aqueous solubility of CNTs.[9] However, the physical interactions between CNTs and ssDNA or pDNA and the nature of such interactions are not well understood, although studied by several techniques.[11,12,16]

Fluorescence spectrophotometry is a technique with high sensitivity and specificity. Moreover, it is nondestructive and has not been widely used for CNT characterization. The UV-vis luminescence of f-CNTs (single- and multiwalled) in liquid phases has been previously reported.[5,17] Such luminescence seems to be an intrinsic property of CNTs, and becomes pronounced following their functionalization.[17a] Riggs et al.[17b] have proposed that the visible luminescence of f-CNTs is due to the extended π-conjugated electronic structure of the carbon backbone and the trapping of excitation energy at various defect sites. More recently, Lin et al.[17c] reported that the better the dispersion and functionalization of the CNTs, the more intense the luminescence emissions observed.

In the present study, we show that f-CNTs (Fig. 1) exhibit distinct excitation and emission spectra in the UV-vis range of the electromagnetic spectrum that can be studied using a standard fluorescence spectrophotometer. The characteristic emission peak of f-CNTs can be used to monitor the extent of CNT-bundle formation and dissociation. Moreover, we investigated how complexation with pDNA in aqueous phases for the purpose of gene-delivery vector construction affects CNT bundling.

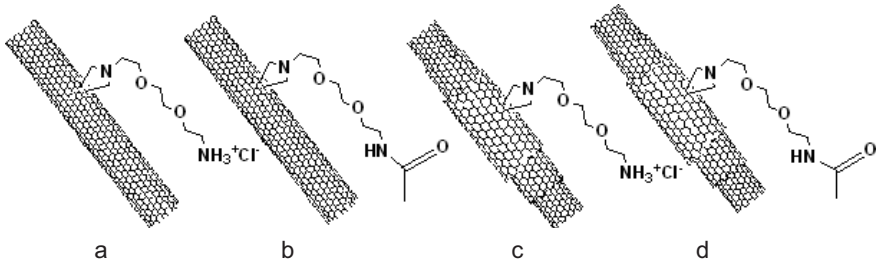

Figure 1. Structures of the f-CNTs used: a) SWNT–NH_3^+, b) SWNT–NH–Ac (NH–Ac: acetamido), c) MWNT–NH_3^+, d) MWNT–NH–Ac.

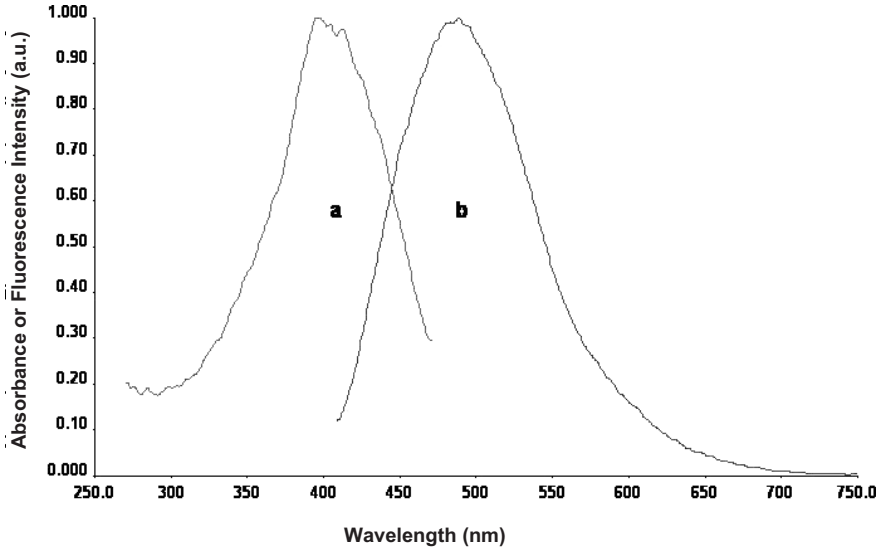

Figure 2. Excitation (a) and emission (b) spectra of 150 μg mL^{-1} SWNT–NH_3^+ in water.

2. Results

2.1. Fluorescence of Aqueous Dispersions of f-CNTs

Figure 2 shows the normalized excitation and emission spectra of an aqueous dispersion of SWNT–NH_3^+ (150 μg mL^{-1}). The excitation spectra of both CNT–NH_3^+ and CNT–NH–Ac (NH–Ac: acetamido) in aqueous dispersions of the same concentration show a broad peak with maximum intensity at 390–395 nm. The emission spectra show maximum intensity peaks at 480–485 nm, indicating a Stokes shift of 90 nm. No remarkable differences were found between the fluorescence intensities of single- and multiwalled CNTs.

Comparing the fluorescence intensity between the two types of functionalizations, the fluorescence intensity obtained from CNT–NH_3^+ was almost twice that obtained from CNT–NH–Ac following excitation at 395 and 390 nm, respectively (Fig. 3II, curves b and d).

2.2. Fluorescence of f-CNTs Dispersed in Sodium Dodecyl Sulfate (SDS) Solutions

Dispersion of f-CNTs in an aqueous phase in the presence of SDS caused an enhancement of the fluorescence intensity of MWNT–NH_3^+ by 20 %, independent of the SDS concentration in the range from 1 to 10 % (w/v) (Fig. 3I). SWNT–NH_3^+ exhibited a similar increase in fluorescence intensity when dispersed in 1 % SDS aqueous solution (Fig. 3II, curves a and b). In accordance with previous studies,[7c,17a,c,18] the observed increases in fluorescence intensity can be attributed to the disruption of nanotube bundles in the liquid phase.

Interestingly, SWNT–NH–Ac exhibited no increase in fluorescence intensity in the presence of SDS (Fig. 3II, curves c and d), indicating that interactions between the surfactant molecules and the nanotubes did not lead to bundle dissociation, as in the case of SWNT–NH_3^+.

2.3. Effect of pH on CNT–NH_3^+ Fluorescence

Aqueous dispersions of MWNT–NH_3^+ had a pH of 4.6 immediately after hydration. At this pH the fluorescence intensity was at its maximum, as shown in Figure 4a. Upon increas-

ADVANCED FUNCTIONAL MATERIALS

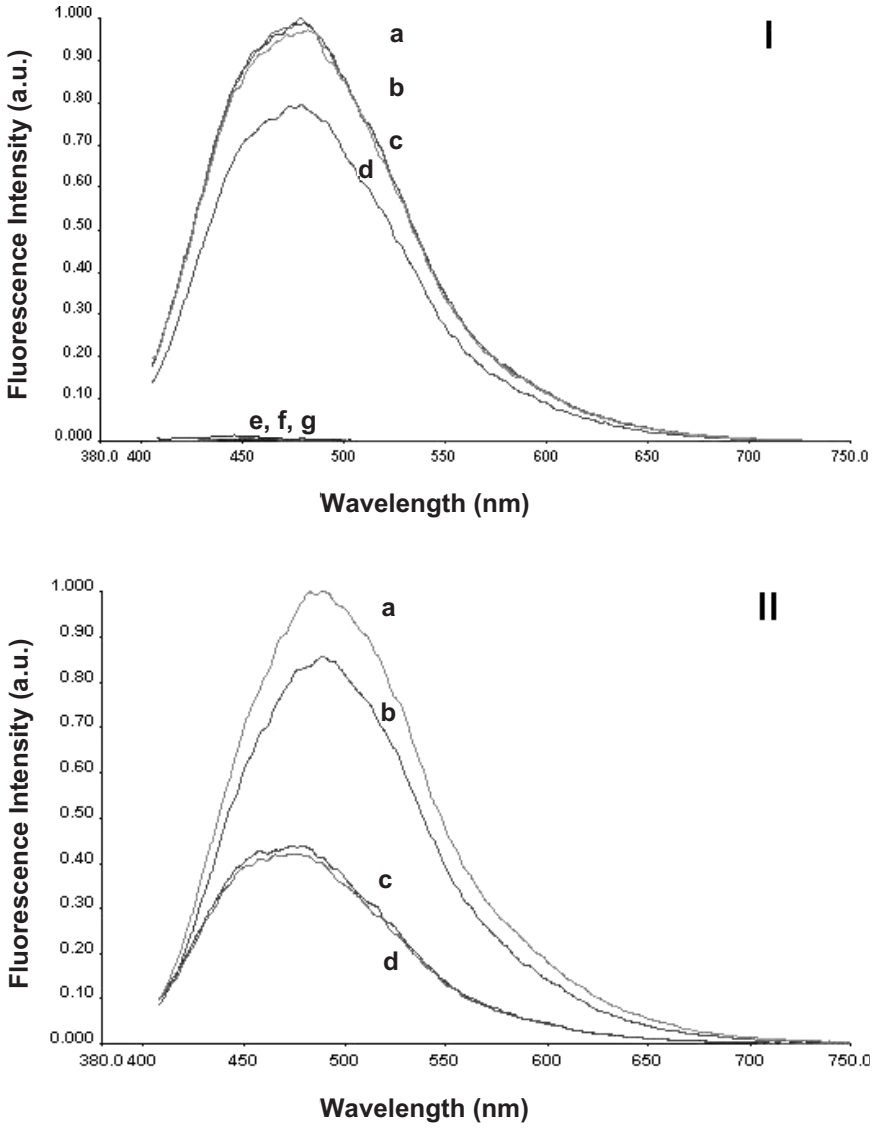

Figure 3. I) Fluorescence spectra of MWNT–NH_3^+ (excitation wavelength, λ_{ex} 390 nm) in a) 1, b) 5, and c) 10% sodium dodecyl sulfate (SDS) aqueous solutions and d) water; and: e) 10, f) 5, and g) 1% aqueous SDS solutions only. II) Fluorescence spectra of SWNT–NH_3^+ (λ_{ex} 395 nm) in 1% SDS and water (a, b), and SWNT–NH–Ac (λ_{ex} 390 nm) in 1% SDS and water (c, d).

ing the pH, the fluorescence of MWNT–NH_3^+ was gradually quenched (Fig. 4). This was an indication that increases in pH led to CNT-bundle formation.

To further elucidate this observation, samples were studied using transmission electron microscopy (TEM). Figure 5 depicts the different degrees of bundling that occurs for MWNT–NH_3^+ at pH 4.6 and 12.0. At pH 4.6 a small number of bundles (aggregates or groups of tubes) could be seen. These bundles are small in dimension, while individual nanotubes seem to be aligned parallel to each other (Fig. 5a and b). In contrast, at pH 12.0 large bundles of MWNT–NH_3^+ are formed with a concurrent aggregation between bundles (Fig. 5c and d). This behavior could be attributed to both the change of pH and the presence of NaCl generated during the titration from acid to basic conditions. Therefore, the observed decrease in fluorescence intensity at higher pH values corresponds to enhanced formation of MWNT–NH_3^+ bundles and bundle aggregates as imaged by TEM.

2.4. Effect of pDNA on f-CNT Fluorescence

Complexation of SWNT–NH_3^+ with pDNA as described previously[11,12] for various pDNA concentrations in aqueous solution produced a gradual quenching of f-CNT fluorescence (Fig. 6). The fluorescence intensity of the SWNT–NH_3^+:pDNA complexes decreased proportionally with increased pDNA concentration.

We can apply the rearranged Stern–Volmer equation:[19]

$$I_0/I - 1 = K\text{sv}\,[\text{quencher}] \qquad (1)$$

(where I_0/I is ratio between the intensities of fluorescence in the absence and presence of the quencher (in our case pDNA), and Ksv is the Stern–Volmer constant) to quantitatively evaluate the efficiency of quenching. Ksv for SWNT–NH_3^+ was calculated to be 9×10^6 M^{-1} (emission at 486 nm), as seen in Figure 7a. However, complexes between MWNT–NH_3^+ and pDNA exhibited a different trend. In the concentration range explored, at low pDNA concentrations a linear relationship with fluorescence quenching was observed, with $K\text{sv} = 2 \times 10^7$ M^{-1} (emission at 480 nm). At higher pDNA concentrations, fluorescence quenching of MWNT–NH_3^+:pDNA complexes reached a plateau, indicating that fluorescence quenching was independent of pDNA concentration (Fig. 7b). In this way, it was quantitatively shown that condensation of pDNA onto f-CNTs led to quenching of their luminescence, indicating bundle formation.

In order to determine the importance of electrostatic interactions in the CNT–NH_3^+:pDNA complex formation and the ensuing quenching effect observed, the fluorescence intensity of complexes prepared from SWNT–NH–Ac and pDNA was studied. As shown in Figure 8, a minor decrease in the luminescence of SWNT–NH–Ac was obtained when complexed with pDNA (curves b and d). This observation indicated that pDNA complexation can lead to minor bundle formation of the SWNT–NH–Ac that may be contributed to by possible hydrophobic interactions between the pDNA and the carbon backbone of the CNTs. SWNT–NH_3^+, on the other hand, exhibits a

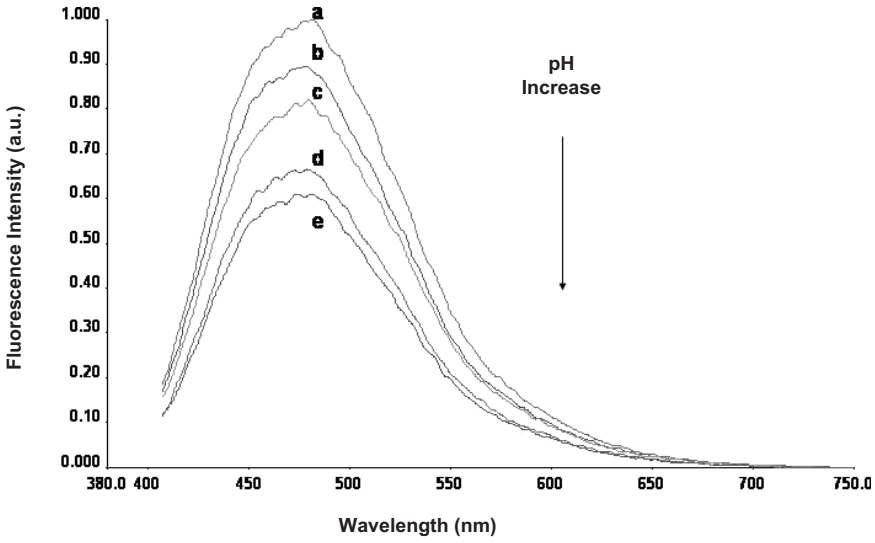

Figure 4. Fluorescence spectra of MWNT–NH_3^+ (λ_{ex} 390 nm) at different pH values: a) 4.6, b) 6.5, c) 8.5, d) 11.5, and e) 12.0. The concentration of MWNT–NH_3^+ was 150 μg mL^{-1}.

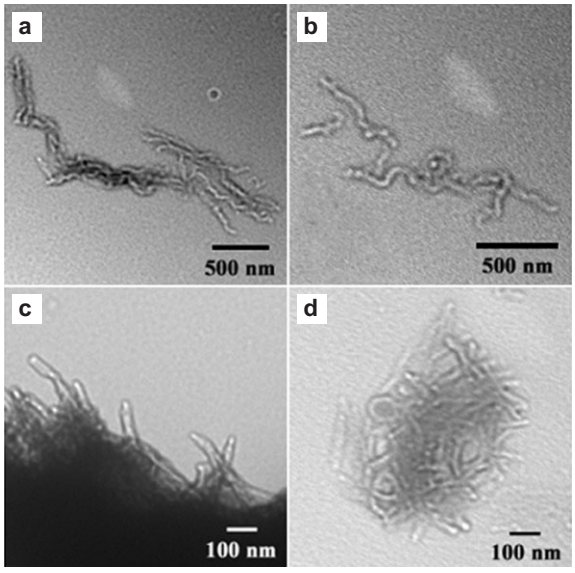

Figure 5. TEM images of 150 μg mL^{-1} MWNT–NH_3^+ tubes in aqueous solution at pH 4.6 (a,b) and pH 12.0 (c,d).

significant decrease in the fluorescence intensity, which is considered an indication of bundle formation (Fig. 8, curves a and c) and the importance of the electrostatic interactions between this type of nanotube and the polyanionic pDNA.

2.5. Effect of SDS on the Complexation of SWNT–NH_3^+ with pDNA

To further investigate whether SDS is capable of interfering with complex formation between SWNT–NH_3^+ and pDNA, or whether it is possible to lead to nanotube-bundle dissociation after formation of the SWNT–NH_3^+:pDNA complex, two experimental protocols were undertaken, as described in the following.

2.5.1. SWNT–NH_3^+:pDNA Complexes Formed in 1 % SDS

To determine if pDNA had the same bundle-formation effect on SWNT–NH_3^+ as that observed in Figure 6 in the presence of SDS, the complexation between pDNA and SWNT–NH_3^+ was performed in a solution of 1 % SDS (Fig. 9d). Comparing the maximum emission peaks of SWNT–NH_3^+ alone (in water and in 1 % SDS), the nanotube fluorescence intensity increased by approximately 20 % in the presence of SDS (Fig. 9, curves a and b) as obtained above (Fig. 3II). The addition of pDNA to SWNT–NH_3^+ dispersed in SDS produced the spectrum shown in Figure 9d, which completely overlaps with the spectrum in Figure 9a, indicating that no change occurred. This data revealed that in SDS solutions the pDNA is unable to condense and form complexes with SWNT–NH_3^+.

2.5.2. SWNT–NH_3^+:pDNA Complexes Diluted in 1 % SDS

Complexes were formed between SWNT–NH_3^+ and 5.3×10^{-8} M pDNA (Fig. 9c). Following addition of SDS to the preformed SWNT–NH_3^+:pDNA complexes (Fig. 9e), luminescence was recovered to the values observed from SWNT–NH_3^+ in SDS (Fig. 9a). This data indicated that SDS was able to compete electrostatically with pDNA for the nanotube surface, resulting in bundle dissociation. Moreover, it confirmed that complexation between SWNT–NH_3^+ and pDNA leads to bundle formation, which can be electrostatically reversed.

3. Discussion

In the present study we propose use of the UV-vis luminescence properties of f-CNTs to monitor their bundle formation and dissociation in aqueous dispersions using standard fluorescence spectrophotometry instrumentation. Moreover, we have applied this tool to better characterize the complexation between f-CNTs and pDNA, which will be essential for future optimization studies of noncovalent complexes between f-CNTs and nucleic acids toward construction of effective CNT-based gene-therapy vectors.[11,12]

Previously, Guldi et al.[5] have shown that triethyleneglycol (TEG)-derivatized CNTs, which result from the 1,3-dipolar cycloaddition reaction, exhibit a quantum yield of 0.4 and emission lifetimes varying from 3.7 to 5.2 ns. The optical features of

ADVANCED FUNCTIONAL MATERIALS

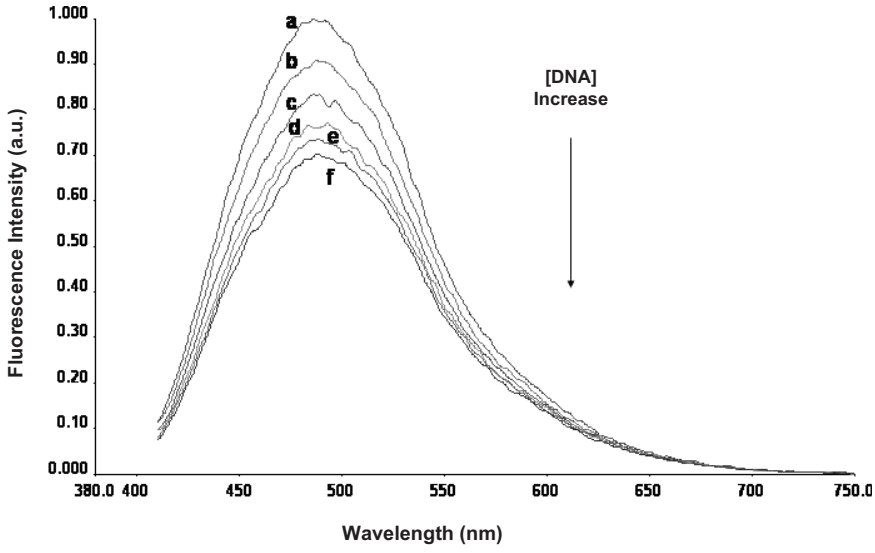

Figure 6. Fluorescence spectra of SWNT–NH_3^+ in water (λ_{ex} 395 nm) alone (a) and in the presence of pDNA at b) 1.1×10^{-8}, c) 2.1×10^{-8}, d) 3.2×10^{-8}, e) 4.2×10^{-8}, and f) 5.3×10^{-8} M. The concentration of SWNT–NH_3^+ was kept constant at 150 μg mL^{-1}.

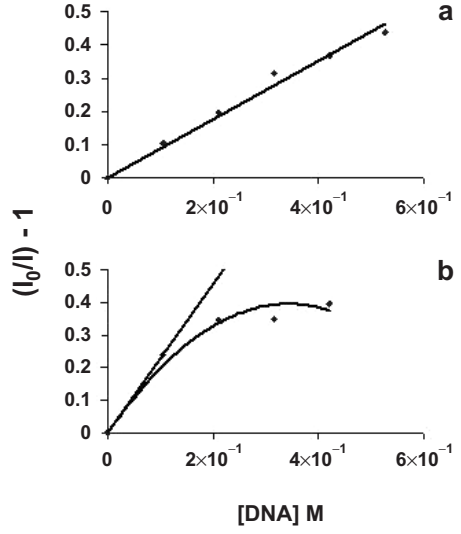

Figure 7. a) Stern–Volmer plot for quenching of the emission of SWNT–NH_3^+ in water (150 μg mL^{-1}; λ_{em} 486 nm) by pDNA. b) Stern–Volmer plot for quenching of the emission of MWNT–NH_3^+ in water (150 μg mL^{-1}; λ_{em} 480 nm) by pDNA.

f-CNTs are expected to be dependent on the chemical moiety with which they are functionalized.[5,17b,c] Our data confirmed such previous observations, as further chemical modification of the TEG-derivatized CNTs to introduce ammonium or acetamido terminal groups (CNT–NH_3^+ and CNT–NH–Ac) led to a significant optical difference between these two types of f-CNTs. The acetamido-functionalized tubes have shown a fluorescence intensity that is half as strong as that of the ammonium-functionalized tubes (Fig. 2).

In order to determine whether nanotube-bundle dissociation can be monitored through the optical properties of f-CNTs we have studied the effect of SDS in aqueous dispersions of f-CNTs. Chen et al.[18] have shown the improved dispersion of acid-treated SWNTs, nonionic-surfactant-coated SWNTs, and acid-treated SWNTs coated with nonionic surfactants after three hours of low-power bath sonication by light scattering. O'Connell et al.[7c] used cup-horn sonication to disperse SDS micelle-coated SWNTs, to find that the photoluminescence intensity of sonicated samples gave more intense emissions in the near-IR region of the electromagnetic spectrum. In agreement with such previously reported studies we found that the dispersion of CNT–NH_3^+ in 1 % SDS aqueous solution assisted by one minute of bath sonication leads to enhanced fluorescence intensity (Fig. 3I). In this way, a proportional relation between fluorescence-intensity enhancement and CNT–NH_3^+ bundle dissociation in water was established.

This observation is thought to occur as SDS disrupts the CNT bundles, therefore more individual CNTs are present in solution, increasing the total CNT surface area and, thus, leading to higher fluorescence intensity. An increase in SDS concentration did not lead to further enhancement of the fluorescence intensity (Fig. 3I). SDS is an amphiphilic molecule with a negatively charged polar head group and a hydrophobic aliphatic chain, while CNT–NH_3^+ are polycationic structures (Fig. 1), with a positive charge from the NH_3^+ functional groups available for ca. every 95 carbon atoms in a polybenzene ring structure.[4] Therefore, these two chemical moieties can, in theory, interact both through hydrophobic and electrostatic forces. The concentration of 1 % SDS used (35 mM) was higher than the critical micelle concentration of this surfactant (8.5 mM);[16a] therefore, SDS is present in the form of micelles. Moreover, the estimated positive/negative charge ratio between the CNTs and SDS was 1:450. We believe that the excess of SDS micelles interact primarily through attractive electrostatic forces with the NH_3^+ groups on the CNT surfaces, allowing for better individualization of nanotubes and stabilization of the CNT–NH_3^+ dispersion. These studies offer previously unreported evidence of CNT-bundle dissociation monitored by UV-vis fluorescence spectrophotometry.

In order to further understand the nature of the interactions between CNT–NH_3^+ and SDS in solution, we studied the fluorescence properties of SWNT–NH–Ac, which possesses an overall neutral surface charge, diluted in a 1 % SDS solution. Figure 3II shows that in a 1 % SDS solution the fluorescence intensity of SWNT–NH–Ac is identical to that in water alone. This observation indicates that the positive charges on the NH_3^+ groups are important sites for interaction with the SDS molecules (particularly their anionic polar heads). Therefore, SDS can result in f-CNT unbundling mainly through electrostatic interactions.

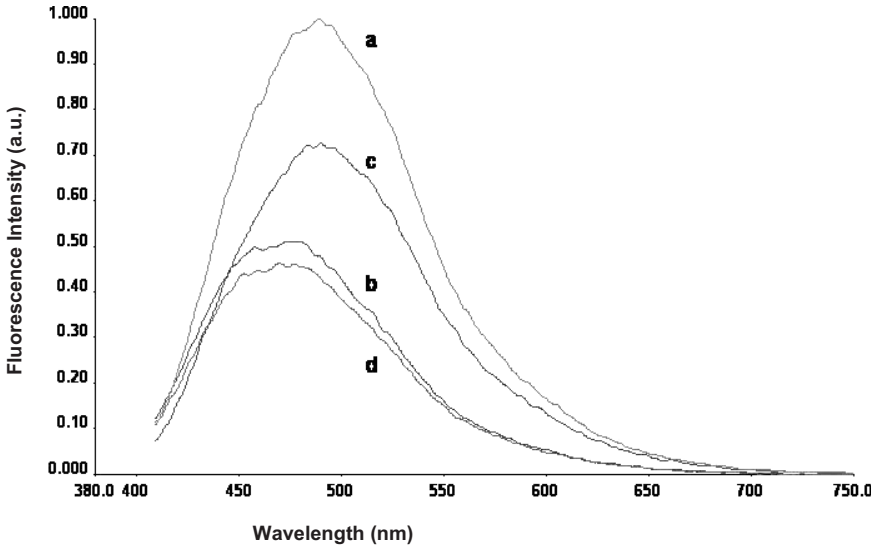

Figure 8. Fluorescence spectra of SWNT–NH_3^+ (λ_{ex} 395 nm) and SWNT–NH–Ac (λ_{ex} 390 nm) in water: alone (a,b, respectively) and complexed with 5.3×10^{-8} M of pDNA (c,d, respectively). The concentration of the f-CNTs was 150 μg mL^{-1} in all cases.

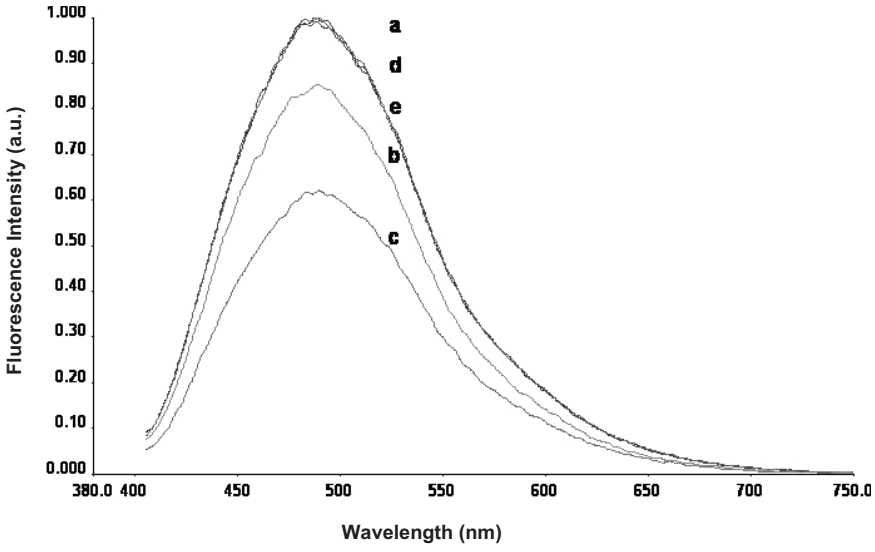

Figure 9. Fluorescence spectra of SWNT-NH_3^+ (λ_{ex} 395 nm) in 1 % SDS (a), in water (b) and complexed with 5.3×10^{-8} M of pDNA (c). Fluorescence spectra of SWNT-NH_3^+ in SDS followed by pDNA complexation (d) and SWNT-NH_3^+:pDNA complexes followed by SDS addition (e). Concentration of SWNT-NH_3^+ left constant at 150 μg mL^{-1} throughout.

The direct relation between fluorescence intensity and bundle formation/dissociation of CNT–NH_3^+ in water was further confirmed by increasing the pH of the dispersion. The functional NH_3^+ groups at the surfaces of the CNTs are introducing electrostatic repulsion forces between nanotubes, enhancing their dispersion. By increasing the pH, the NH_3^+ groups were gradually neutralized, resulting in increased bundle formation and bundle aggregation (Figs. 4 and 5). This phenomenon was accompanied by a decrease in fluorescence intensity (quenching). Decrease to pH 2 did not lead to further enhancement in fluorescence intensity, indicating that the nanotubes were adequately individualized and dispersed in the aqueous buffer at pH 4.6. We therefore obtained evidence confirming the correlation between bundle formation (by pH increase) and dissociation (by addition of SDS) from UV-vis fluorescence intensity.

Previously, we explored the physicochemical interactions between f-CNTs and DNA during complex formation in studies that focused on the characteristics of pDNA condensation and the ensuing supramolecular complexes.[12] In the present study, we attempted to elucidate how pDNA can affect or change the aggregation status of CNT–NH_3^+ in bulk solution using much higher CNT–NH_3^+:pDNA charge ratios. Zheng et al.[9] have reported that ssDNA assisted the dispersion and separation of bundled, non-functionalized SWNTs in water by sonication. We found that an excess of ds-pDNA can lead to quenching of CNT–NH_3^+ fluorescence, signifying increased f-CNT bundle formation (Fig. 6). With regards to the nature of such interactions, the data obtained here are in complete agreement with our previously reported observations.[12] The supramolecular complex formed between CNT–NH_3^+ and pDNA is stabilized by strong electrostatic interactions. However, we can not exclude contributions from hydrophobic interactions that can also allow the pDNA to aggregate CNTs. Such hydrophobic interactions may be responsible for the moderate quenching obtained when the neutral SWNT–NH–Ac were allowed to complex with pDNA (Fig. 8). The pDNA-mediated f-CNT bundling can be explained by either neutralization of the positive charges at the f-CNT surface, leading to reduction of the repulsive forces between neighboring tubes, or, alternatively, by the ability of pDNA to form CNT bundles by wrapping around multiple tubes.

Concerning the strength of the CNT–NH_3^+:pDNA association, we have observed that in the presence of SDS (independent of the order of addition to the f-CNT and their complexes with pDNA) unbundling of the tubes was achieved. Others have also suggested a modest binding of calf thymus ssDNA to non-functionalized CNTs solubilized with SDS.[16a] This study has shown (Fig. 9) that SDS micelles compete with the nucleic acid and are capable of displacing pDNA from the positively charged f-CNT surfaces, leading to increased nanotube individualization. Therefore, the binding between CNT–NH_3^+ and pDNA is reversible, indicating that release of the plasmid from the nanotube surface is

ADVANCED FUNCTIONAL MATERIALS

possible. This finding is particularly important for gene-delivery applications of such complexes, since release of the condensed nucleic acid is required intracellularly to achieve gene expression or silencing.

4. Conclusion

Very recently, the high sensitivity of UV-vis luminescence obtained from a series of functionalized CNTs has been proposed as a valuable tool in the evaluation of their dispersion and aggregation state in aqueous media.[17c] We have shown herein that fluorescence spectrophotometry in the UV-vis region is indeed a reliable and accurate technique by which to characterize the aggregation and self-assembly of aqueous dispersions of f-CNTs, particularly after complexation with other macromolecules such as surfactants, polymers, or nucleic acids. Utilization of f-CNTs as gene-delivery systems will require a better understanding of the complexes formed between f-CNTs and nucleic acids. This study showed that f-CNT:pDNA complex formation is taking place primarily through electrostatic interactions, leading to enhanced nanotube-bundle formation and aggregation. These observations have direct implications as far as the pharmacological and therapeutic capabilities of such complexes are concerned. Their degree of aggregation will have a decisive role on their in vivo pharmacokinetic profile (interaction with blood and complementary-system components) and their interactions with target cells (cellular binding and intracellular trafficking), which will ultimately determine therapeutic efficacy. We propose that the luminescence properties of f-CNTs and fluorescence spectrophotometry be used as a standardized methodology by which to monitor the aggregation of biologically compatible CNTs towards development of these materials as nanomedicines.

5. Experimental

Aqueous Dispersions of f-CNTs: SWNTs were purchased from Carbon Nanotechnologies Inc. (Houston, TX). Pristine SWNTs used in this experiment were CNI Grade/Lot No. R0496. According to the supplier, the median diameter of the SWNTs is about 1 nm. Tube lengths are between 300 and 1000 nm, although this is difficult to determine because the tubes organize themselves into ropes. MWNTs were purchased from Nanostructured and Amorphous Materials Inc. (Houston, TX). MWNTs used in this experiment were 94 % pure, outer diameter: 20–30 nm, stock No. 1240XH. The length is between 0.5 and 2 μm. Water-soluble ammonium-functionalized SWNTs (SWNT–NH_3^+) and MWNTs (MWNT–NH_3^+) (Fig. 1) were synthesized by organic functionalization as previously reported [4]. The concentration of available functional groups (NH_3^+) on the SWNT and MWNT surfaces was determined using the quantitative Kaiser test to be 0.5 and 0.6 mmol g^{-1} of material, respectively [4]. SWNT–NH–Ac were prepared by solubilizing 5 mg of CNT–NH_3^+ in 600 μL of dimethylformamide (DMF) and adding 200 μL of acetic anhydride. The solution was stirred for 1.5 h and then precipitated several times in cold diethyl ether. The qualitative Kaiser test was negative. Stock dispersions were prepared by hydration of CNT–NH_3^+ in deionized water at concentrations of 6 mg mL^{-1} (SWNT). SWNT–NH–Ac were hydrated at a concentration of 6 mg mL^{-1}. All dispersions were kept at 4 °C until needed.

Plasmid DNA: A gigaprep of highly purified supercoiled pDNA (pCMV-βgal, BD-Clontech, UK) was prepared by Bayou Biolabs (LA, USA). A stock solution was prepared in deionized water at a concentration of 1 mg mL^{-1}. Aliquots were stored frozen at –80 °C until needed.

Sodium Dodecyl Sulfate: A stock aqueous solution of 10 % SDS (BDH Laboratories Supplies, UK) was prepared with deionized water. Dilutions of 5 and 1 % of SDS were obtained from the stock solution.

f-CNT Dispersions in SDS: Samples with 150 μg mL^{-1} of CNT–NH_3^+ (single- and multiwalled) were prepared by dilution of the appropriate volume of the aqueous f-CNT stock dispersions in 1, 5, and 10 % solutions of SDS. All samples were bath sonicated at 45 kHz (Ultrasonic Cleaner, VWR International, UK) for one minute (to aid the homogenization of the dispersion) and left at room temperature for 30 min before the fluorescence spectra were collected. Samples of 150 μg mL^{-1} of SWNT–NH–Ac were prepared following the same protocol.

pH Modification of Aqueous CNT–NH_3^+ Dispersions: Samples of 150 μg mL^{-1} of CNT–NH_3^+ (single- and multiwalled) were prepared by dilution of appropriate volumes of the stock CNT dispersion with deionized water. The pH of the CNT–NH_3^+ dispersions as prepared was 4.6 (ISFET pH meter KS 701, Camlab, UK). The pH of each sample was modified by drop wise addition of 0.02 M HCl or NaOH.

f-CNT:DNA Complexes: Samples of CNT–NH_3^+ (single- and multiwalled) were prepared by dilution of appropriate volumes of the stock dispersion with deionized water to reach a volume of 0.5 mL. Serial dilutions of pDNA in volumes of 0.5 mL (final concentrations from 1.05 to 5.3×10^{-8} M) were prepared from the aqueous stock solution. Each solution of pDNA (0.5 mL) was added to a sample of CNT–NH_3^+ (0.5 mL) and the mixture was rapidly pipetted ten times. Complexes were allowed to form for 30 min at room temperature and then diluted to a final volume of 2 mL with deionized water. The final concentration of CNT–NH_3^+ was 150 μg mL^{-1}. Complexes between SWNT–NH–Ac and pDNA (5.3×10^{-8} M final concentration) were prepared following the protocol described above.

SWNT–NH_3^+:pDNA Complexes Formed in 1 % SDS: SWNT–NH_3^+ were first diluted in SDS and then complexed with pDNA following the protocol described above.

SWNT–NH_3^+:pDNA Complexes Diluted in 1 % SDS: SWNT–NH_3^+:pDNA complexes were prepared in water as described above and then SDS was added to a final concentration of 1 % w/v. In both cases, all samples were left for 30 min at room temperature following addition of the third component. Final concentrations of each component were as follows: 150 μg mL^{-1} of SWNT–NH_3^+, 5.3×10^{-8} M of pDNA, and 1 % of SDS.

UV-Vis Excitation and Fluorescence Spectra: The excitation and emission spectra were obtained with a LS-50B spectrophotometer (Perkin Elmer, UK). All spectra were normalized to the maximum peak of each set, equivalent to 1.0 arbitrary units (a.u.) of fluorescence intensity.

Transmission Electron Microscopy: Aqueous samples containing MWNT–NH_3^+ at pH 4.6 and 12.0 were deposited in 300-mesh copper grids coated with formvar/carbon support film (Euromedex). Previously, the grids were "glow discharged" in an Emitech K350G system (Emitech Ltd.) for 3 min at 30 mA (negative polarity). Imaging was carried out with a Philips 208 transmission electron microscope working at different accelerating voltages. Pictures were taken using a high-resolution CCD (CCD: charge-coupled device) camera (AMT, Eindhoven, The Netherlands) at an accelerating voltage of 120 kV. Digital images were captured using an AMT high-resolution camera. The preparation of the samples was as follows: 300 μg of MWNT were solubilized in 1 mL of milliQ H_2O. The pH was modified using 0.02 M HCl and 0.05 M NaOH solutions added dropwise. When the desired pH was achieved, the samples were completed to a final volume of 2 mL. The final concentration of the f-CNT samples was 150 μg mL^{-1}.

Received: August 24, 2005
Final version: February 13, 2006
Published online: August 16, 2006

[1] S. Iijima, *Nature* **1991**, *354*, 56.
[2] R. Saito, G. Dresselhaus, M. S. Dresselhaus, *Physical Properties of Carbon Nanotubes*, Imperial College Press, London **1998**.
[3] a) A. Bianco, K. Kostarelos, C. D. Partidos, M. Prato, *Chem. Commun.* **2005**, 571. b) W. A. de Heer, *MRS Bull.* **2004**, *29*, 281.
[4] a) V. Georgakilas, K. Kordatos, M. Prato, D. M. Guldi, M. Holzinger, A. Hirsch, *J. Am. Chem. Soc.* **2002**, *124*, 760. b) V. Georgakilas, N. Tagmatarchis, D. Pantarotto, A. Bianco, J. P. Briand, M. Prato, *Chem. Commun.* **2002**, 3050.
[5] D. M. Guldi, M. Holzinger, A. Hirsch, V. Georgakilas, M. Prato, *Chem. Commun.* **2003**, 1130.
[6] R. Shvartzman-Cohen, Y. Levi-Kalisman, E. Nativ-Roth, R. Yerushalmi-Rozen, *Langmuir* **2004**, *20*, 6085.
[7] a) A. Hartschuh, H. N. Pedrosa, L. Novotny, T. D. Krauss, *Science* **2003**, *301*, 1354. b) M. S. Strano, C. A. Dyke, M. L. Usrey, P. W. Barone, M. J. Allen, H. W. Shan, C. Kittrell, R. H. Hauge, J. M. Tour, R. E. Smalley, *Science* **2003**, *301*, 1519. c) M. J. O'Connell, S. M. Bachilo, C. B. Huffman, V. C. Moore, M. S. Strano, E. H. Haroz, K. L. Rialon, P. J. Boul, W. H. Noon, C. Kittrell, J. P. Ma, R. H. Hauge, R. B. Weisman, R. E. Smalley, *Science* **2002**, *297*, 593.
[8] G. R. Dieckmann, A. B. Dalton, P. A. Johnson, J. Razal, J. Chen, G. M. Giordano, E. Munoz, I. H. Musselman, R. H. Baughman, R. K. Draper, *J. Am. Chem. Soc.* **2003**, *125*, 1770.
[9] M. Zheng, A. Jagota, E. D. Semke, B. A. Diner, R. S. McLean, S. R. Lustig, R. E. Richardson, N. G. Tassi, *Nat. Mater.* **2003**, *2*, 338.
[10] Y. Sabba, E. L. Thomas, *Macromolecules* **2004**, *37*, 4815.
[11] D. Pantarotto, R. Singh, D. McCarthy, M. Erhardt, J. P. Briand, M. Prato, K. Kostarelos, A. Bianco, *Angew. Chem. Int. Ed.* **2004**, *43*, 5242.
[12] R. Singh, D. Pantarotto, D. McCarthy, O. Chaloin, J. Hoebeke, C. D. Partidos, J. P. Briand, M. Prato, A. Bianco, K. Kostarelos, *J. Am. Chem. Soc.* **2005**, *127*, 4388.
[13] a) C. Dwyer, M. Guthold, M. Falvo, S. Washburn, R. Superfine, D. Erie, *Nanotechnology* **2002**, *13*, 601. b) H. Xin, A. T. Woolley, *J. Am. Chem. Soc.* **2003**, *125*, 8710.
[14] a) M. L. Guo, J. H. Chen, D. Y. Liu, L. H. Nie, S. Z. Yao, *Bioelectrochemistry* **2004**, *62*, 29. b) J. Wang, G. Liu, M. R. Jan, *J. Am. Chem. Soc.* **2004**, *126*, 3010.
[15] L. W. Chen, C. L. Cheung, P. D. Ashby, C. M. Lieber, *Nano Lett.* **2004**, *4*, 1725.
[16] a) J. Rajendra, M. Baxendale, L. G. Dit Rap, A. Rodger, *J. Am. Chem. Soc.* **2004**, *126*, 11 182. b) E. Buzaneva, A. Karlash, K. Yakovkin, Y. Shtogun, S. Putselyk, D. Zherebetskiy, A. Gorchinskiy, G. Popova, S. Prilutska, O. Matyshevska, Y. Prilutskyy, P. Lytvyn, P. Scharff, P. Eklund, *Mater. Sci. Eng. C* **2002**, *19*, 41. c) O. P. Matyshevska, A. Y. Karlash, Y. V. Shtogun, A. Benilov, Y. Kirgizov, K. O. Gorchinskyy, E. V. Buzaneva, Y. I. Prylutskyy, P. Scharff, *Mater. Sci. Eng. C* **2001**, *15*, 249. d) G. I. Dovbeshko, O. P. Repnytska, E. D. Obraztsova, Y. V. Shtogun, *Chem. Phys. Lett.* **2003**, *372*, 432.
[17] a) Y. P. Sun, B. Zhou, K. Henbest, K. F. Fu, W. J. Huang, Y. Lin, S. Taylor, D. L. Carroll, *Chem. Phys. Lett.* **2002**, *351*, 349. b) J. E. Riggs, Z. X. Guo, D. L. Carroll, Y. P. Sun, *J. Am. Chem. Soc.* **2000**, *122*, 5879. c) Y. Lin, B. Zhou, R. B. Martin, K. B. Henbest, B. A. Harruff, J. E. Riggs, Z. X. Guo, L. F. Allard, Y. P. Sun, *J. Phys. Chem. B* **2005**, *109*, 14 779. d) Y. Sun, S. R. Wilson, D. I. Schuster, *J. Am. Chem. Soc.* **2001**, *123*, 5348. e) Y. P. Sun, W. J. Huang, Y. Lin, K. F. Fu, A. Kitaygorodskiy, L. A. Riddle, Y. J. Yu, D. L. Carroll, *Chem. Mater.* **2001**, *13*, 2864. f) S. Banerjee, S. S. Wong, *J. Am. Chem. Soc.* **2002**, *124*, 8940. g) N. Nagasawa, H. Sugiyama, N. Naka, I. Kudryashov, M. Watanabe, T. Hayashi, I. Bozovic, N. Bozovic, G. Li, Z. Li, Z. K. Tang, *J. Lumin.* **2002**, *97*, 161. h) X. Xu, R. Ray, Y. Gu, H. J. Ploehn, L. Gearheart, K. Raker, W. A. Scrivens, *J. Am. Chem. Soc.* **2004**, *126*, 12 736.
[18] Q. Chen, C. Saltiel, S. Manickavasagam, L. S. Schadler, R. W. Siegel, H. Yang, *J. Colloid Interface Sci.* **2004**, *280*, 91.
[19] L. H. Chen, D. McBranch, R. Wang, D. Whitten, *Chem. Phys. Lett.* **2000**, *330*, 27.